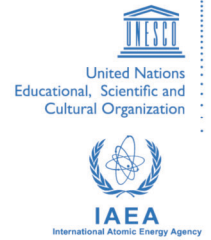




**The Abdus Salam
International Centre for Theoretical Physics**



1968-2

Conference on Teleconnections in the Atmosphere and Oceans

17 - 20 November 2008

On the Role of Atmospheric Teleconnections in Climate.

Anastasios A. TSONIS
*Atmospheric Sciences Group
Dept. of Mathematical Sciences
University of Wisconsin
Milwaukee
USA*

On the Role of Atmospheric Teleconnections in Climate

ANASTASIOS A. TSONIS AND KYLE L. SWANSON

Atmospheric Sciences Group, Department of Mathematical Sciences, University of Wisconsin—Milwaukee, Milwaukee, Wisconsin

GELI WANG

Institute of Atmospheric Physics, Chinese Academy of Sciences, Beijing, China

(Manuscript received 21 February 2007, in final form 29 October 2007)

ABSTRACT

In a recent application of networks to 500-hPa data, it was found that supernodes in the network correspond to major teleconnection. More specifically, in the Northern Hemisphere a set of supernodes coincides with the North Atlantic Oscillation (NAO) and another set is located in the area where the Pacific–North American (PNA) and the tropical Northern Hemisphere (TNH) patterns are found. It was subsequently suggested that the presence of atmospheric teleconnections make climate more stable and more efficient in transferring information. Here this hypothesis is tested by examining the topology of the complete network as well as of the networks without teleconnections. It is found that indeed without teleconnections the network becomes less stable and less efficient in transferring information. It was also found that the pattern chiefly responsible for this mechanism in the extratropics is the NAO. The other patterns are simply a linear response of the activity in the tropics and their role in this mechanism is inconsequential.

1. Introduction

This work uses methods from graph theory to investigate the role of teleconnection in climate. Because these methods are new to the atmospheric sciences community we begin with an introduction of the basic ideas. Some of these basic principles have been presented in a recent publication (Tsonis et al. 2006), but are presented here as well for convenience and completeness.

A network is a system of interacting agents. In the literature an agent is called a node. The nodes in a network can be anything. For example, in the network of actors, the nodes are actors that are connected to other actors if they have appeared together in a movie. In a network of species the nodes are species that are connected to other species they interact with. In the network of scientists, the nodes are scientists that are connected to other scientists if they have collaborated.

In the grand network of humans each node is an individual, which is connected to people he or she knows. There are four basic types of networks.

a. Regular (ordered) networks

These networks are networks with a fixed number of nodes, each node having the same number of links connecting it in a specific way to a number of neighboring nodes (Fig. 1, left panel). If each node is linked to all other nodes in the network, then the network is a fully connected network. When the number of links per node is high, regular networks have a high (local) clustering coefficient. In this case accidental removal of a number of links does not break the network into noncommunicating parts; the network is stable, which may not be the case for regular networks with small local clustering. Also, unless networks are fully wired, they have a large diameter. The diameter of a network is defined as the maximum shortest path between any pair of its nodes. It relates to the characteristic path-length, which is the average number of links in the shortest path between two nodes. The smaller the diameter, the easier the communication is in the network.

Corresponding author address: A. A. Tsonis, Department of Mathematical Sciences, Atmospheric Sciences Group, University of Wisconsin—Milwaukee, Milwaukee, WI 53201.
E-mail: aatsonis@uwm.edu

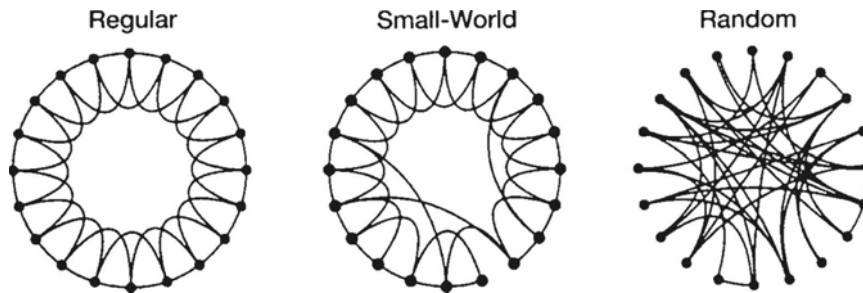


FIG. 1. Illustration of a regular, a small-world, and a random network (after Watts and Strogatz 1998).

b. Classical random networks

In these networks the nodes are connected at random (Fig. 1, right panel). In this case the degree distribution is a Poisson distribution (the degree distribution, p_k , gives the probability that a node in the network is connected to k other nodes). The problem with these networks is that they have very small clustering coefficient and thus not very stable. Removal of a number of nodes at random, may fracture the network to noncommunicating parts. On the other hand, they are characterized by a small diameter. Faraway nodes can be connected as easily as nearby nodes. In this case, information may be transported all over the network much more efficiently than in ordered networks. Thus, random networks exhibit efficient information transfer, but they are not stable.

c. Small-world networks

In nature we should not expect to find either very regular or completely random networks. Rather we should find networks that would be efficient in processing information and at the same time be stable. Work in this direction led to a new type of network, which was proposed a few years ago by the American mathematicians Watts and Strogatz (1998) and is called *small-world* network. A “small-world” network is a superposition of regular and classical random graphs. Such networks exhibit a high degree of local clustering but a small number of long-range connections make them as efficient in transferring information as random networks. Those long-range connections do not have to be designed. A few long-range connections added at random will do the trick (Fig. 1, middle panel). The degree distribution of small-world networks is also a Poisson distribution.

d. Networks with a given degree distribution

The small-world architecture can explain phenomena such as the six degrees of separation (most people are

friends with their immediate neighbors, but we all have one or two friends a long way away), but it really is not a model found often in the real world. In the real world the architecture of a network is neither random nor small world, but it comes in a variety of distributions such as truncated power-law distributions, Gaussian distributions, power-law distributions, and distributions consisting of two power laws separated by a cutoff value (for a review see Strogatz 2001). The most interesting and common of such networks are the so-called *scale-free* networks. Consider a map showing an airline’s routes. This map has a few hubs connecting with many other points (i.e., supernodes) and many points connected to only a few other points, a property associated with power-law distributions. Such a map is highly clustered, yet it allows motion from a point to another faraway point with just a few connections. As such, this network has the *property* of small-world networks, but this property is not achieved by local clustering and a few random connections. It is achieved by having a few elements with a large number of links and many elements having very few links. Thus, even though they share the same property, the architecture of scale-free networks is different than that of small-world networks. Such inhomogeneous networks have been found to pervade biological, social, ecological, and economic systems, the Internet, and other systems (Albert et al. 1999; Liljeros et al. 2001; Jeong et al. 2001; Pastor-Satorras and Vespignani 2001; Bouchaud and Mezard 2000; Barabási and Bonabeau 2003). These networks are referred to as scale free because they show a power-law distribution of the number of links per node. Lately, it was also shown that, in addition to the power-law degree distribution, many real scale-free networks consist of self-repeating patterns on all length scales (Song et al. 2005). These properties are very important because they imply some kind of self-organization within the network. Scale-free networks are not only efficient in transferring information, but due to the high degree of local clustering they are also very stable

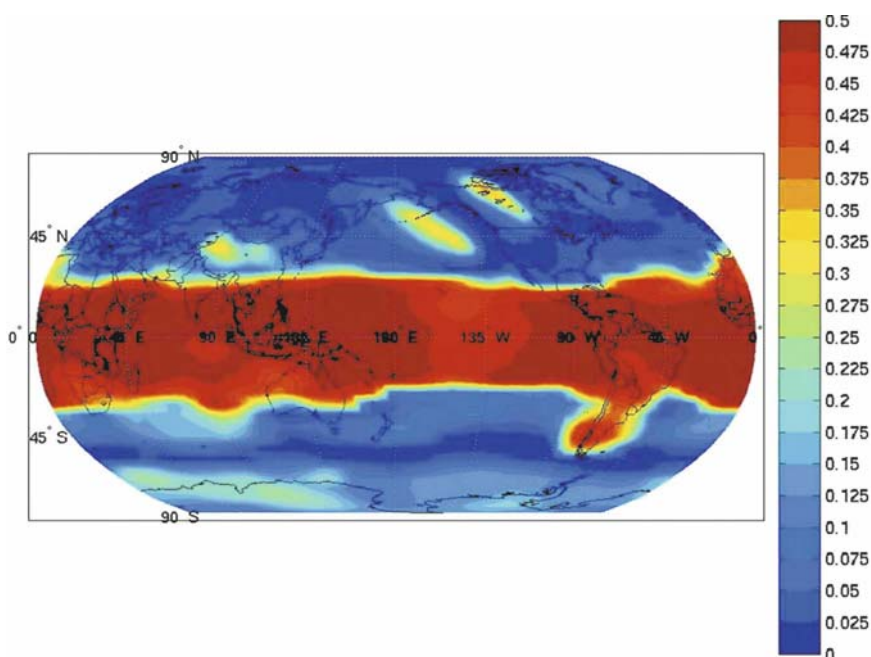


FIG. 2. Total number of links (connections) at each geographic location. The uniformity observed in the tropics indicates that each node possesses the same number of connections. This is not the case in the extratropics where certain nodes possess more links than the rest. See text for details on how this figure was produced.

(Barabási and Bonabeau 2003). Because there are only a few supernodes, chances are that accidental removal of some nodes will not include the supernodes. In this case the network would not become disconnected. This is not the case with weakly connected regular or random networks (and to a lesser degree with small-world networks), where accidental removal of the same percentage of nodes makes them more prone to failure (Barabási and Bonabeau 2003).

2. Previous results

Methods to construct networks were applied to the climate system by assuming that climate is represented by a grid of oscillators each one of them representing a dynamical system varying in some complex way. The goal was to delineate the collective behavior of these interacting dynamical systems and the structure of the resulting network (Tsonis and Roebber 2004; Tsonis et al. 2006). They considered the global National Centers for Environmental Prediction–National Center for Atmospheric Research (NCEP–NCAR) reanalysis 500-hPa dataset (Kistler et al. 2001). A 500-hPa value indicates the height of the 500-hPa pressure level and provides a good representation of the general circulation (wind flow) of the atmosphere. The resolution of the data in those studies was 5° latitude \times 5° longitude.

For each grid point a time series of monthly anomaly values in the period December–February from 1950 to 2004 is available. In this network each grid point is a node and two nodes are considered as connected if the absolute value of the correlation coefficient of their respective time series is greater or equal to 0.5. The architecture of the resulted network is presented in Fig. 2, which shows the area-weighted number of total links (connections) at each geographic location. More accurately it shows the fraction of the total global area that a point is connected to. This is a more appropriate way to show the architecture of the network because the network is a continuous network defined on a sphere. Thus, if a node i is connected to N other nodes at λ_N latitudes then its area-weighted connectivity, \tilde{C}_i , is defined as

$$\tilde{C}_i = \frac{\sum_{j=1}^N \cos \lambda_j}{\sum_{\text{over all } \lambda \text{ and } \varphi} \cos \lambda}, \quad (1)$$

where φ is the longitude. In the above expression the denominator is the area of the earth's surface and the numerator is the area of that surface a node is connected to. We observe two very interesting features. In the tropics, it appears that all nodes possess more or less the same (and high) number of connections, which is a characteristic of fully connected networks. In the extra-

tropics, it appears that certain nodes possess more connections than the rest, which is a characteristic of scale-free networks. In the Northern Hemisphere we clearly see the presence of regions where such supernodes exist in China, North America, and the northeast Pacific Ocean. Similarly several supernodes are visible in the Southern Hemisphere. These differences between the tropics and extratropics have been delineated in the corresponding degree distributions, which suggest that indeed the extratropical network is a scale-free network characterized by a power-law degree distribution (Tsonis et al. 2006). As is the case with all scale-free networks, the extratropical network is also a small-world network (Tsonis et al. 2006).

An interesting observation in Fig. 2 is that supernodes may be associated with major teleconnection patterns. For example, the supernodes in North America and the northeast Pacific Ocean are located where the well-known Pacific–North American (PNA) pattern (Wallace and Gutzler 1981) is found. In the Southern Hemisphere we also see supernodes over the southern tip of South America, Antarctica, and the south Indian Ocean that are consistent with some of the features of the Pacific–South American (PSA) pattern (Mo and Higgins 1998). Interestingly, no such supernodes are evident where the other major pattern, the North Atlantic Oscillation (NAO; Thompson and Wallace 1998; Pozo-Vázquez et al. 2001; Huang et al. 1998) is found. This does not indicate that NAO is not a significant feature of the climate system. Since NAO is not strongly connected to the tropics, the high connectivity of the tropics with other regions is masking NAO out. In fact, if we consider a network with only nodes north of the 30°N latitude, we find (Fig. 3, top) that features consistent with NAO are not only present but are also the prominent features of the network (the other two panels of Fig. 3 are discussed later). It should be noted here that in their pioneering paper Wallace and Gutzler (1981) defined teleconnectivity at each grid point as the strongest negative correlation between a grid point and all other points. This brings out teleconnection patterns associated with waves such as the trough–ridge–trough PNA pattern. However, because of the requirement of strongest negative correlation (which occurs between a negative anomaly center and a positive anomaly center), this approach can only delineate long-range connections. As such, information about clustering and connectivity at other spatial scales is lost. In the network approach all the links at a point are considered and as such much more information (clustering coefficients, diameter, scaling properties, etc.) can be obtained. The similarities between Wallace and Gutzler's results and the network results arise from the fact that

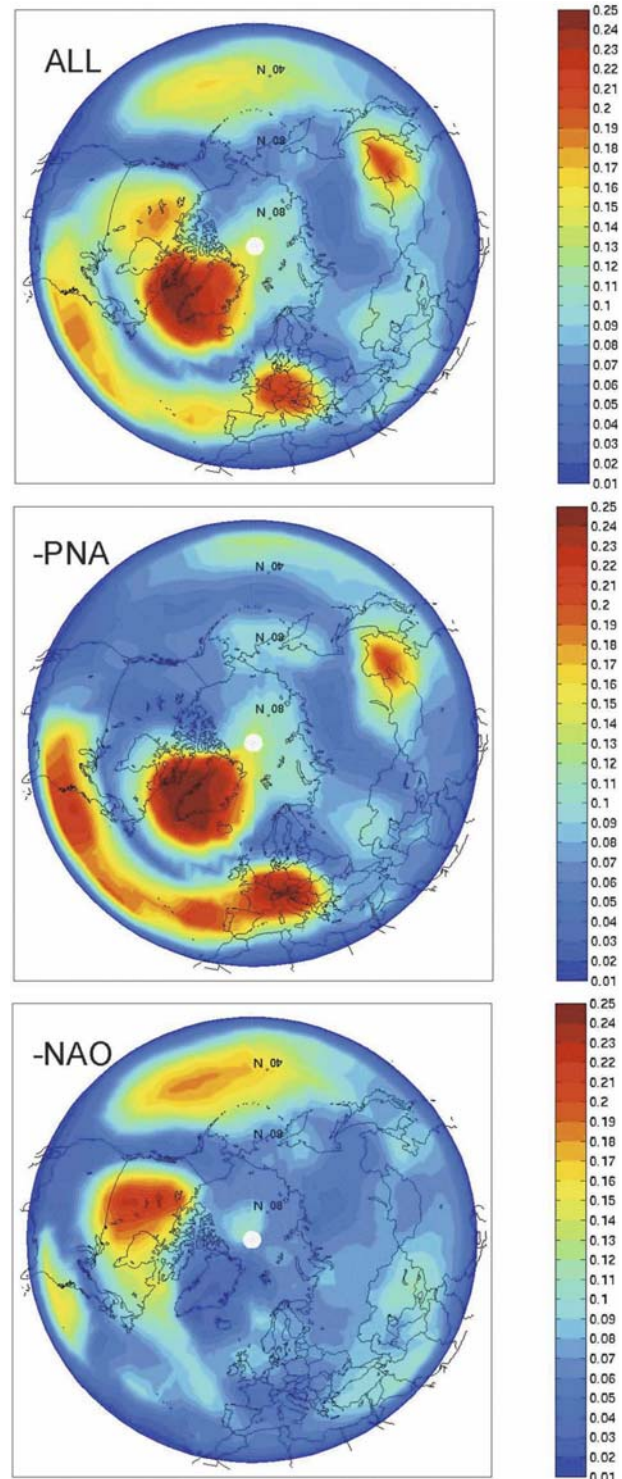


FIG. 3. (top) Same as in Fig. 2, but for the extratropical network (30°–90°N). (middle) Same as in (top), but for the network without PNA. (bottom) Same as in (top), but for the network without NAO.

grid points with many long-range links will most likely stand out. The network approach, however, appears superior as it is able to delineate both major teleconnection patterns at once.

The mathematical terminology of networks and graph theory may appear rather abstract but is often associated with the physics of the system the network represents or is applied to. For example, networks of nonlinear oscillators may synchronize and experience bifurcations as physical parameters vary (Pecora et al. 1997; Boccaletti et al. 2002; Tsonis et al. 2007). The rate at which the degree (number of links) of each node changes is equivalent to thermodynamics forces and their conjugated flows and to Onsager relations, which explain how small perturbations of some parameters can induce fluctuations of other parameters (Fronczak et al. 2007). With regards to our previous results mentioned above and the new results presented here, the physical interpretation is that the climate system (as represented by the 500-hPa field) exhibits properties of stable networks and of networks where information is transferred efficiently. In the case of the climate system, “information” should be regarded as “fluctuations” from any source. These fluctuations will tend to destabilize the source region. For example, dynamical connections between the ocean and the atmosphere may create a disturbance in the upper-atmospheric flow from a surface temperature anomaly over the Pacific Ocean. However, the small world as well as the scale-free property of the extratropical network allows the system to respond quickly and coherently to fluctuations introduced into the system. This information transfer diffuses local fluctuations thereby reducing the possibility of prolonged local extremes and providing greater stability for the global climate system. The above theory and its application to climate data suggest that the climate system may be inherently stable and efficient in transferring information and that these properties are closely connected to the presence of teleconnections. Next we present results that further document this hypothesis.

3. Results

Empirical orthogonal function (EOF) analysis is a well-known procedure in the atmospheric sciences, which “decomposes” a signal into modes (EOFs) of variability. Each mode explains some of the variance observed in the data. The first EOF explains most of the variance, and so on. Figure 4 shows the first and second EOF of the extratropical (30° – 90° N) 500-hPa field. Here the data in the period December–March at a resolution of $2.5^{\circ} \times 2.5^{\circ}$ are used. Figure 4 is consis-

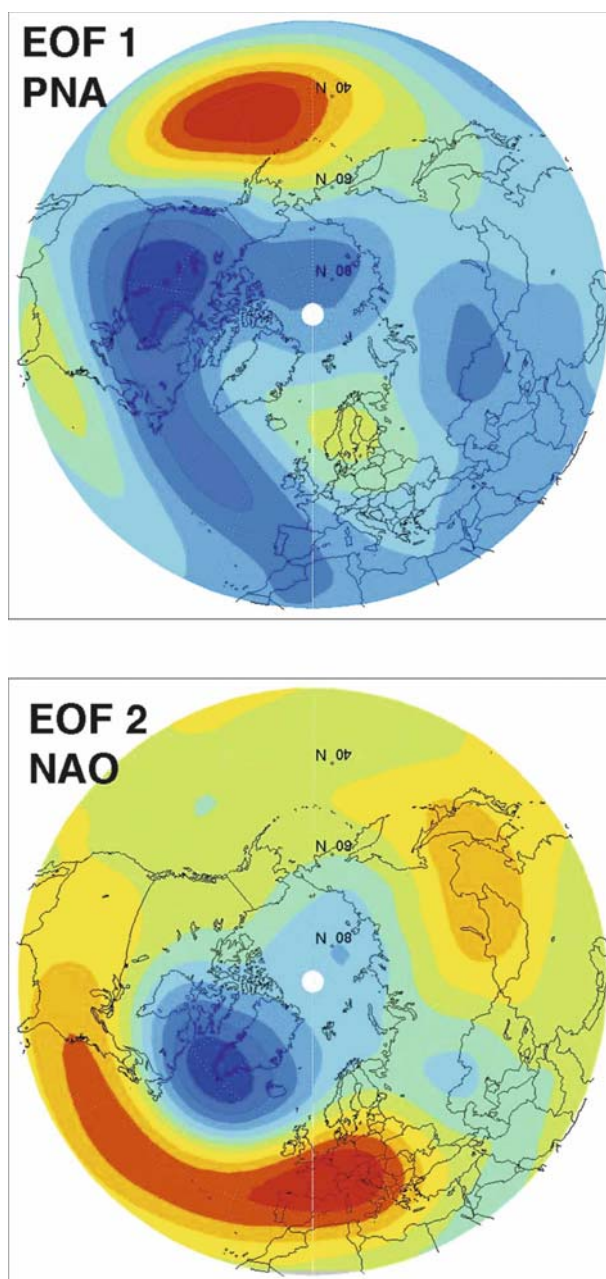


FIG. 4. EOF1 and EOF2 of the observed extratropical 500-hPa flow. The correlations between the NAO and PNA indices and the corresponding temporal components (PCA loadings) are close to 0.9 whereas between TNH and the corresponding temporal component, the correlation is 0.6. Thus, in our case EOF1 identifies more closely the PNA rather than TNH.

tent with previous studies suggesting that these first two EOFs correspond to NAO and PNA. In our case EOF1 corresponds to the PNA pattern, and EOF2 to the NAO, albeit the difference in variance explained is very small (16% and 14%, respectively). We note that EOF patterns that explain similar percentage variances may

not be uniquely defined. Also some studies have suggested that EOF1 identifies the tropical Northern Hemisphere (TNH) pattern (Straus and Shukla 2002). However, in our case we find that the correlations between the NAO and PNA indices and their corresponding temporal components [i.e., the principal component analysis (PCA) loadings] are close to 0.9 whereas between TNH and its corresponding temporal component is 0.6. Thus, in our case EOF1 identifies more closely the PNA rather than TNH. In any case, whether it is the PNA or the TNH that associates with EOF1 is not crucial to the approach here (this will become evident below). We also note here that depending on the period used and the type of data, EOF1 may not always correspond to PNA. For example, if 700-hPa data are used, EOF1 corresponds to NAO (whose presence is more pronounced the closer we are to the surface) and EOF2 corresponds to PNA but again in this case the difference in variance explained is very small about 20% and 17%, respectively [Van den Dool et al. (2000); see also the early work of Wallace and Gutzler (1981)]. The interesting feature of EOF analysis is that we can use the results to approximate the original data by including only EOFs that contribute significantly to total variance. In this process we can exclude one significant mode (PNA or NAO) to construct new data without that mode. This way we can construct a climate without the PNA pattern or without the NAO. As such we have a procedure to investigate how climate will behave without the presence of one or more major teleconnection patterns. Having the reconstructed climates we can then investigate the variability of their networks and isolate the role of teleconnections (i.e., supernodes in the network) in climate.

The bottom two panels in Fig. 3 show the reduced climate networks (without PNA and without NAO, respectively). In addition to these connectivity maps, Fig. 5 shows the total distance for each grid point, which is the average length of all its links multiplied by its connectivity (for reference, the distance between the equator and the Pole is $\pi/2$).¹ Table 1 shows the clustering coefficient and the average distance of the network for the complete and the reduced networks. The average total distance of the network is the average of the corresponding field in Fig. 5. It relates to the diameter of the network; the larger the distance the smaller the diameter the easier the information transfer.

Before discussing the interpretation of these results, it is useful to revisit the procedure of estimating the clustering coefficient. The procedure to estimate the

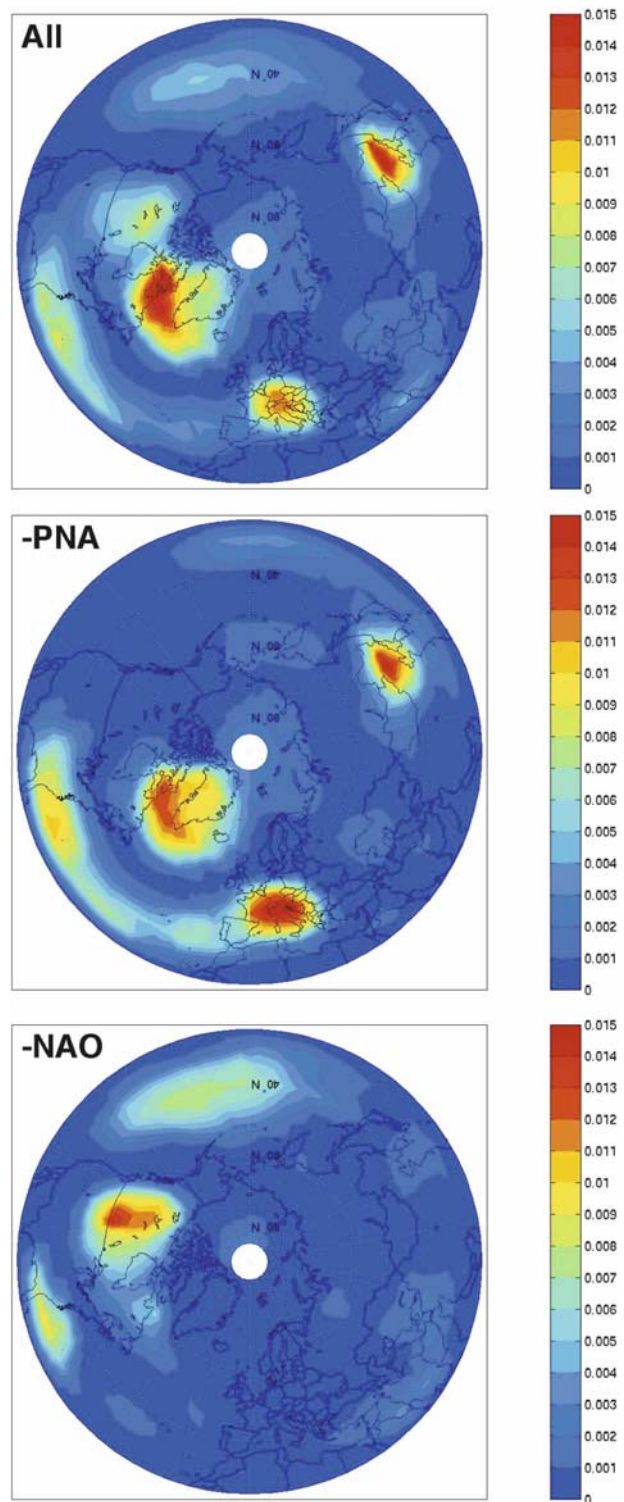


FIG. 5. Total distance at each geographical location (top) for the complete network, (middle) for the network without PNA, and (bottom) for the network without NAO. See text for definition of distance.

¹ Here $\pi/2$ = Pole-to-equator distance.

TABLE 1. Clustering coefficient and distance for the networks considered.

	Modified clustering coefficient	Distance
Complete network	0.34	0.0025
Network without PNA	0.33	0.0023
Network without NAO	0.27	0.0016

clustering coefficient in classical networks is illustrated in Fig. 6. The top panel shows a hypothetical network and the links of a specific node (the central one, in this case denoted as i). According to this information the central point is connected to eight other nodes. These eight nodes are called the *neighbors* of node i and define the *closest neighborhood* of this node. To estimate the clustering coefficient for this node we then find the number of distinct links between these eight neighbors, Δ_i . For any number of k_i neighbors there are at most $k_i(k_i - 1)/2$ possible connections. This happens when each node in the neighborhood is connected to every other node in the neighborhood (the central point is not part of the neighborhood). In our example there are five links between the neighbors. Thus $\Delta_i = 5$. Then, the clustering coefficient for node i is $C_i = 2\Delta_i / (k_i - 1)k_i = 0.178$ (Watts and Strogatz 1998). Based on this definition the clustering coefficient varies between $[0, 1]$. The

average C_i over all nodes provides the clustering coefficient of the network, C . For a fully connected network $C = 1$ and for a random network $C = \langle k \rangle / N$, where $\langle k \rangle$ is the average number of links per node and N is the total number of nodes in the network.

The above definition of the clustering coefficient is appropriate for classical networks where the relative position of nodes and links is arbitrary and there are no spatial correlations between nearby nodes (e.g., a network of scientists where a link indicates that the two corresponding scientists have coauthored a paper). In our case, the network is derived from a spatially extended system where local spatial correlations extending up to some characteristic scale as well as long-range spatial correlations are present. Indeed, we find that in such cases removal of the supernodes does not change the clustering coefficient. When we remove a supernode we effectively remove its long-range links while background local correlations still remain. In this case the neighborhood becomes smaller but it may still be well connected (because of the local correlations), which means that the clustering coefficient after removing the supernodes may not decrease as expected in classical nonspatial networks. To account for this adverse effect we have introduced a variation of the definition of the clustering coefficient (Tsonis et al. 2006, 2008). This modified procedure is outlined in Fig. 7. The top-left panel shows again a hypothetical 2D uniform grid (where now each grid represents a square of some area and where spatial correlations between grid

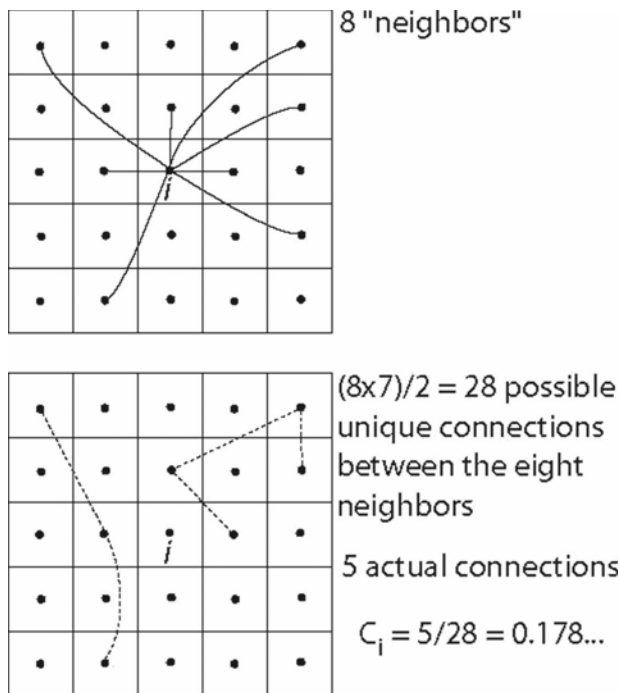


FIG. 6. Illustration of the method to estimate the clustering coefficient (see text for details).

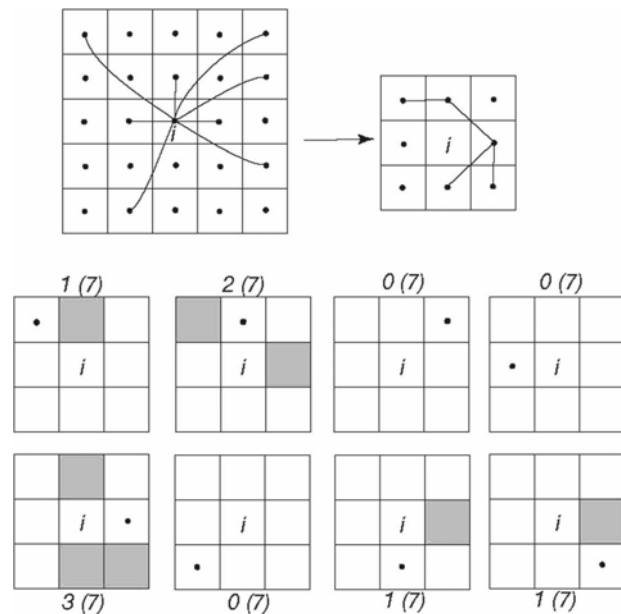


FIG. 7. Illustration of the method to estimate the modified clustering coefficient (see text for details).

points may exist) and the links of the central node i . According to this information the central point is connected to eight other nodes. This means that $\tilde{C}_i = 8/25$. This number is specific to the central node and we use it to define the size of the closest *in space* neighborhood to the central node, which, accordingly, will be the closest eight squares shown on the top-right panel. This panel also shows all the links between the representative grid points in this neighborhood (again here the central point is not part of the neighborhood). The bottom eight panels correspond to the eight neighbors and show the area each grid point is connected to. For example, the first of these eight panels corresponds to the top-left neighbor and shows the area on the grid that it is connected to (i.e., the black square). This number, (e.g., 1), is indicated on the top of this panel. The number in the parenthesis, (e.g., 7), is the maximum number of squares that each node could be connected to. Doing this for all eight neighbors we find that the neighbors are connected to a sum of eight squares. Dividing this number by the maximum sum possible (8×7 squares) gives the clustering coefficient of the central node, 0.1428. More formally, the modified clustering coefficient for a node i is defined as $C_{mi} = 2\Delta_{mi}/(k_i - 1)k_i$, where Δ_{mi} is the number of distinct links (four in the above illustration) between pairs of nodes in the closest spatial neighborhood of node i defined by \tilde{C}_i , and $k_i(k_i - 1)/2$ is the maximum number of possible distinct links between k_i nodes (28 in our illustration). Based on this definition the clustering coefficient varies again between $[0, 1]$. The average C_{mi} over all nodes provides the modified clustering coefficient of the network, C_m . The above procedure can easily be extended to the surface of a sphere with the help of Eq. (1). Note that because we are now calculating on the earth's surface north of 30°N , the area provided by \tilde{C}_i may not always be a circle, but it could be some arc sector. Note also that the presence of spatial correlations does not adversely affect the estimation of the diameter (or distance) of the network.

The results in Table 1 indicate that both the modified clustering coefficient and the average distance of the network without PNA are virtually unchanged compared to the complete network, whereas in the network without NAO they are significantly smaller (20% and 36%, respectively). Here we need to stress the following: as we mentioned above, when the long-range links due to teleconnections are removed, the closest spatial neighborhood for the nodes associated with supernodes becomes smaller. One may argue then that the clustering coefficient will increase because the local correlations cause most of nodes in a small neighborhood to be connected, which will indicate that after the removal of

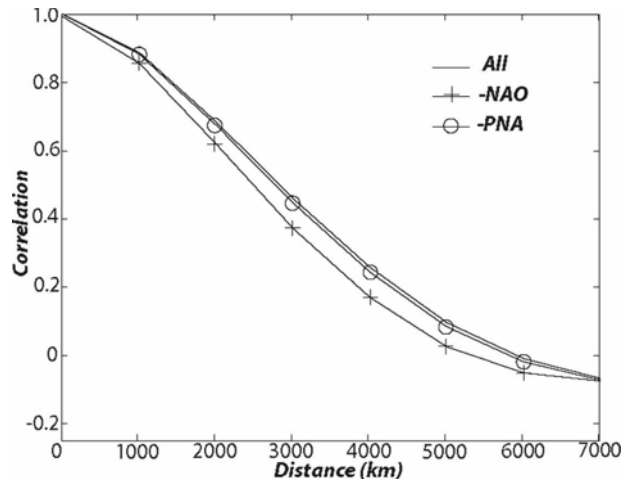


FIG. 8. For the 500-hPa field used here this figure shows the average correlation between two points as a function of their distance, for the complete field, and for the fields without PNA and without NAO. When the PNA is removed we see that the local correlation structure remains unchanged. However, when NAO is removed the local correlation structure weakens.

the supernodes the system becomes more locally clustered and thus more stable rather than the other way around. It follows that in order to be consistent with graph theory, which demands that removal of supernodes makes the network less connected and less stable (i.e., with a smaller clustering coefficient), the removal of a supernode has to also *weaken local correlations*. This conjecture is verified by the data. Figure 8 shows for the 500-hPa field used here the average correlation between two points as a function of their distance, for the complete field and for the fields without PNA and without NAO. We see that when the PNA is removed the local correlation structure remains unchanged. However, when NAO is removed the local correlation structure weakens, which should result in a more fragmented network. This novel result is consistent with the definition of the modified clustering coefficients in Table 1, and indicates that the modified approach to estimate the clustering coefficient in spatially extended systems is more appropriate.

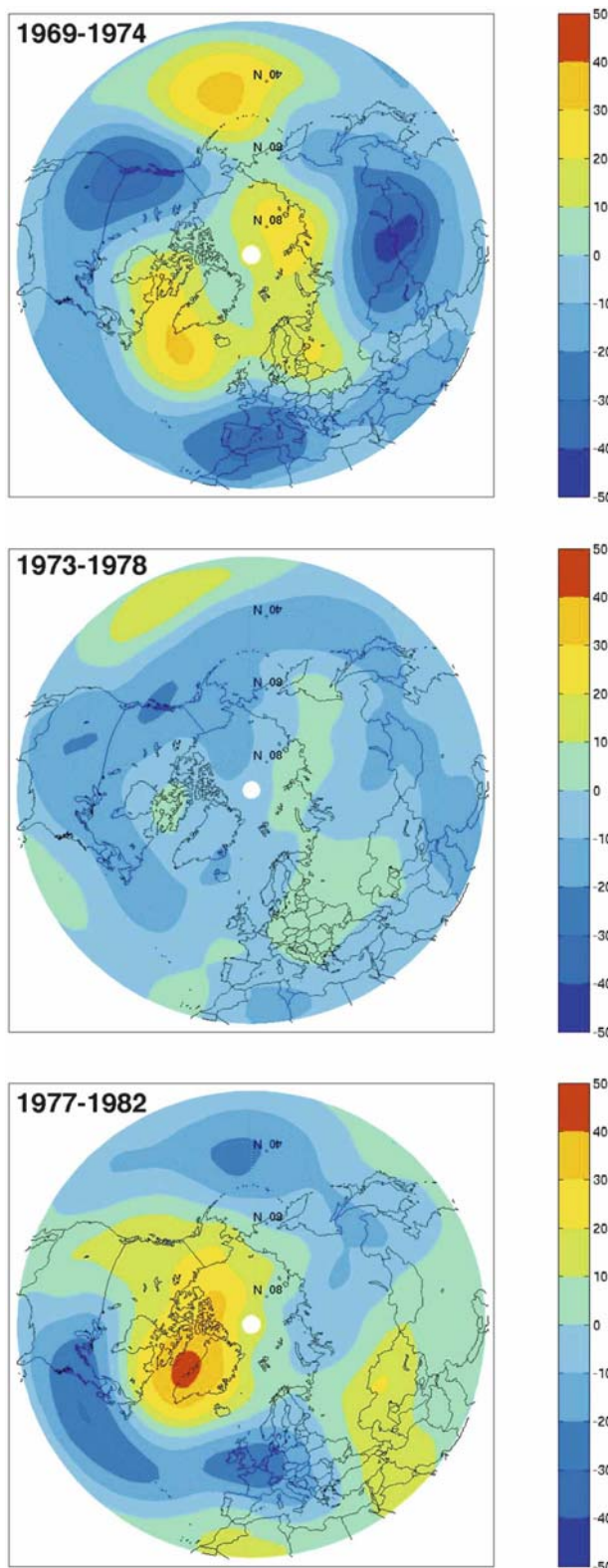
The above results point to the following. 1) The PNA is not relevant to the stability and efficiency of the climate network in the extratropics. Given that in the global network (Fig. 2) the PNA is the major feature in the Northern Hemisphere extratropics, this result indicates that the PNA pattern is a linear response to tropical forcing. In other words, most of its connections are with the tropics and not with the extratropics. 2) On the other hand, the NAO is the pattern that appears to be the major force in the extratropics. These points can be visualized in Figs. 2, 3, and 5. In the global network

(Fig. 2) the PNA pattern stands out whereas NAO is virtually absent. In the extratropics-only network (Figs. 3 and 5) the PNA has “faded” and NAO dominates. The small connectivity and total distance of the extratropical network observed in the areas of the PNA pattern is an indication that only local small-scale connections or connections within itself are associated with this pattern, whereas points associated with NAO have much longer range. The results in Figs. 2, 3, and 4 are not affected by the time window (December–March) used. Different windows produce similar networks and properties.

As we discussed in the introduction a lower clustering coefficient means that the network is becoming more prone to failure and a greater diameter (i.e., a smaller distance) implies less efficient transfer of information. Here we see that when the true supernodes (the NAO) are removed, the network becomes less clustered locally and less efficient in transferring information. This will indicate that the climate network from a stable and efficient scale-free–small-world network becomes a not so highly clustered regular network. Now the network is more prone to failure and thus not as stable. In this case “failure” will indicate the breakdown of a prolonged regime and the emergence of a new regime. This, directly suggested from graph theory, conjecture is verified from observations. Figure 9 shows 500-hPa anomaly composites for three 5-yr periods in the 1970s and early 1980s. In the early 1970s (top panel) the 500-hPa anomaly field is dominated by the presence of a wave-3 pattern with both the PNA and NAO (in its negative phase) being very pronounced. In the mid-1970s (middle panel) this field is very weak and both NAO and PNA have for all practical purposes disappeared. After that (bottom panel), the field becomes strong again but a new wave-2 pattern with a very pronounced positive NAO has emerged. This shift is known as the climate shift of the 1970s. This event is clearly consistent with our hypothesis. When supernodes are removed climate becomes unstable and shifts to a new state. Lately, Tsonis et al. (2007) have discov-

→

FIG. 9. The 500-hPa anomaly field composites for the period (top) 1969–74, (middle) 1973–78, and (bottom) 1977–82. In the (top) a wave-3 pattern is visible with PNA and NAO in its negative phase being present. In the (middle) both NAO and PNA have for all practical purposes disappeared. In the (bottom) the field emerges as a wave-2 pattern with NAO in its positive phase. As we explain in the text this transition (known as the climate shift of the 1970s) is consistent with our conjecture that removal of supernodes makes the network (i.e., the climate) unstable and more prone to failure (i.e., the breakdown of a regime and emergence of another regime).



ered a dynamical mechanism explaining such shifts. According to that study major climate modes may synchronize. Once in place, the synchronized state may become unstable and shift to a new state. It appears that our conjecture plays a role in this desynchronization of major climate modes. This point is the subject of our continuing work in this area and more results will be forthcoming in the future.

As a final note we would like to point out that EOF2 (representing NAO) includes, apart from the dipole over western Europe and Greenland, a third center east of Mongolia. Other EOF-type analyses have also featured this center in the EOF delineating NAO (Van den Dool et al. 2000). This center, which is also visible in the connectivity map (Fig. 3, top), does not appear to be associated with the weak and dubious western Pacific pattern. This may indicate that the NAO actually is a three-pole pattern rather than a dipole. The fact that this center is absent in the global network (Fig. 2), where NAO is suppressed due to its lack of connections with the tropics, provides support to this hypothesis. Our analysis also brings up the more general question as to whether or not EOF analysis (which is based on variance explained) is indeed the appropriate method to study climate signals or oscillations. EOF analysis associates the first EOF with the PNA pattern while in the network approach NAO is far more dominant. Thus, if variance is more important than how the system works (i.e., underlying topology), then EOF analysis may be the best approach. Otherwise, approaches like the network approach may be more appropriate. We have started looking into this problem and more details may be forthcoming in future publications.

Finally we note that the above results are highly reproduced in model simulations. Figures 10, 11, and 12 are similar to Figs. 3, 4, and 5, respectively, but for the 300-yr ECHAM5/Max Planck Institute Ocean Model (MPI-OM) model simulation from Max Planck Institute for Meteorology. While differences in magnitudes can be observed, qualitatively all major features in the results from observations are reproduced in the results from the simulation. This indicates that the results from the observations are not due to inhomogeneities in the NCEP-NCAR reanalysis or length of data.

4. Conclusions

Atmospheric teleconnections are very intriguing phenomena in the climate system. The dynamics underlying the establishment of teleconnections are not well understood. Here we have used a novel approach to study the role of atmospheric teleconnection in climate. We find that teleconnections in the extratropics play

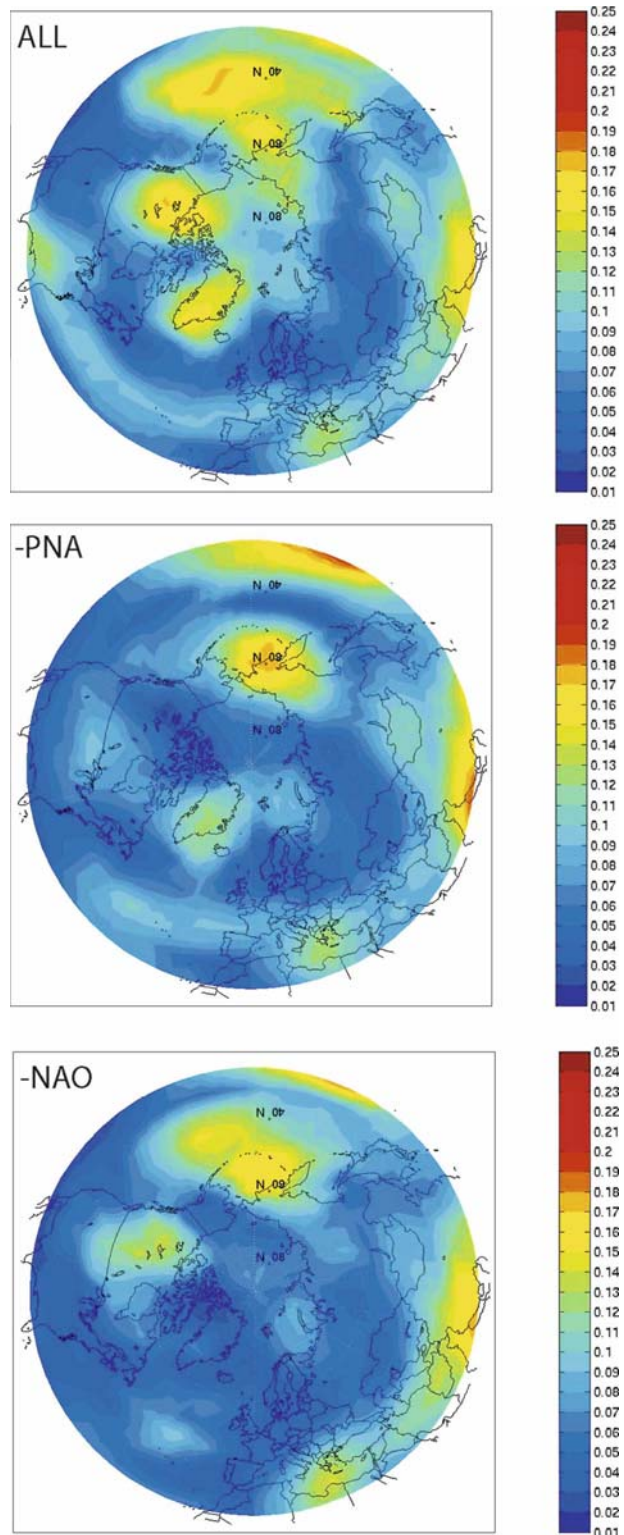


FIG. 10. Same as in Fig. 3, but for the 300-yr ECHAM5/MPI-OM simulation.

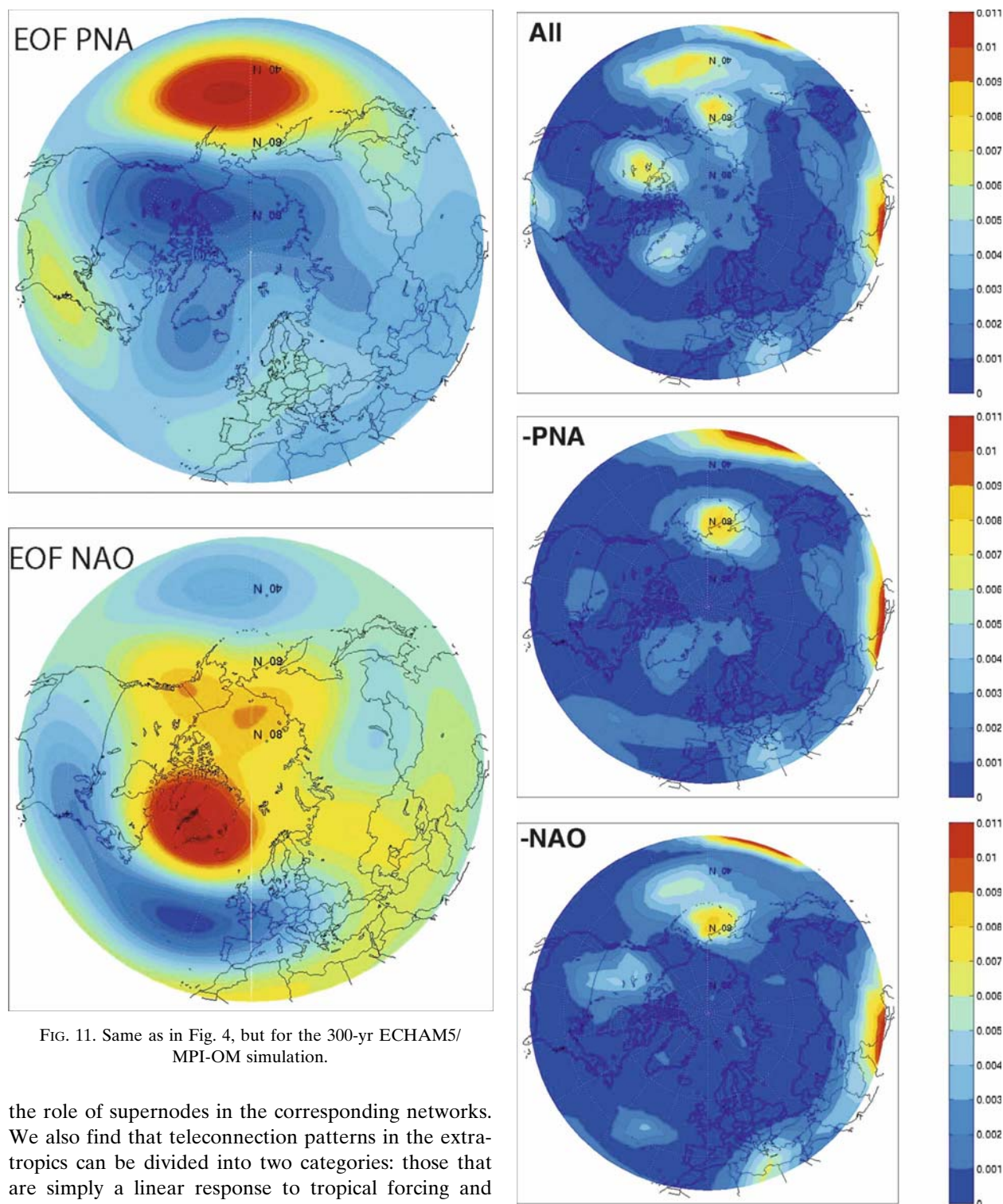


FIG. 11. Same as in Fig. 4, but for the 300-yr ECHAM5/MPI-OM simulation.

the role of supernodes in the corresponding networks. We also find that teleconnection patterns in the extratropics can be divided into two categories: those that are simply a linear response to tropical forcing and those that are intrinsic to the extratropics. Finally, we verify the hypothesis that teleconnections make climate more stable and more efficient in transferring information; removal of the dominant supernodes results in less stable and less efficient networks thus increasing the chances for a major climate shift.

FIG. 12. Same as in Fig. 5, but for the 300-yr ECHAM5/MPI-OM simulation.

Acknowledgments. This work was supported by NSF Grant ATM-0438612 to AAT and KLS, by an UWM RGI grant to AAT, and by NSFC Grant 40505018 to GW.

REFERENCES

- Albert, R., H. Jeong, and A.-L. Barabási, 1999: Internet: Diameter of the World-Wide Web. *Nature*, **401**, 130–131.
- Barabási, A.-L., and E. Bonabeau, 2003: Scale-free networks. *Sci. Amer.*, **288**, 60–69.
- Boccaletti, S., J. Kurths, G. Osipov, D. J. Valladares, and C. S. Zhou, 2002: The synchronization of chaotic systems. *Phys. Rep.*, **366**, 1–101.
- Bouchaud, J.-P., and M. Mezard, 2000: Wealth condensation in a simple model of economy. *Physica A*, **282**, 536–540.
- Fronczak, A., P. Fronczak, and J. A. Holyst, 2007: Thermodynamic forces, flows, and Onsager coefficients in complex networks. *Phys. Rev. E*, **76**, 061106, doi:10.1103/PhysRevE.76.061106.
- Huang, J. P., K. Higuchi, and A. Shabbar, 1998: The relationship between the North Atlantic Oscillation and El Niño–Southern Oscillation. *Geophys. Res. Lett.*, **25**, 2707–2710.
- Jeong, H., S. Mason, A.-L. Barabási, and Z. N. Oltvai, 2001: Lethality and centrality in protein networks. *Nature*, **411**, 41–42.
- Kistler, R., and Coauthors, 2001: The NCEP–NCAR 50-Year Reanalysis: Monthly means CD-ROM and documentation. *Bull. Amer. Meteor. Soc.*, **82**, 247–267.
- Liljeros, F., C. Edling, L. A. Nunes Amaral, H. E. Stanley, and Y. Åberg, 2001: The web of human sexual contacts. *Nature*, **411**, 907–908.
- Mo, K. C., and R. W. Higgins, 1998: The Pacific–South American modes and tropical convection during the Southern Hemisphere winter. *Mon. Wea. Rev.*, **126**, 1581–1596.
- Pastor-Satorras, R., and A. Vespignani, 2001: Epidemic spreading in scale-free networks. *Phys. Rev. Lett.*, **86**, 3200–3203.
- Pecora, L. M., T. L. Carroll, G. A. Johnson, D. J. Mar, and J. F. Heagy, 1997: Fundamentals of synchronization in chaotic systems, concepts, and applications. *Chaos*, **7**, 520–543.
- Pozo-Vázquez, D., M. J. Esteban-Parra, F. S. Rodrigo, and Y. Castro-Díez, 2001: The association between ENSO and winter atmospheric circulation and temperature in the North Atlantic region. *J. Climate*, **14**, 3408–3420.
- Song, C., S. Havlin, and H. A. Makse, 2005: Self-similarity of complex networks. *Nature*, **433**, 392–395.
- Straus, D. M., and J. Shukla, 2002: Does ENSO force the PNA? *J. Climate*, **15**, 2340–2358.
- Strogatz, S. H., 2001: Exploring complex networks. *Nature*, **410**, 268–276.
- Thompson, D. W. J., and J. M. Wallace, 1998: The Arctic Oscillation signature in the wintertime geopotential height and temperature fields. *Geophys. Res. Lett.*, **25**, 1297–1300.
- Tsonis, A. A., and P. J. Roebber, 2004: The architecture of the climate network. *Physica A*, **333**, 497–504.
- , K. L. Swanson, and P. J. Roebber, 2006: What do networks have to do with climate? *Bull. Amer. Meteor. Soc.*, **87**, 585–595.
- , —, and S. Kravtsov, 2007: A new dynamical mechanism for major climate shifts. *Geophys. Res. Lett.*, **34**, L13705, doi:10.1029/2007GL030288.
- , —, and G. Wang, 2008: Estimating the clustering coefficient in scale-free networks on lattices with local correlation structure. *Physica A*, in press.
- Van den Dool, H. M., S. Saha, and A. Johansson, 2000: Empirical orthogonal teleconnections. *J. Climate*, **13**, 1421–1435.
- Wallace, J. M., and D. S. Gutzler, 1981: Teleconnections in the geopotential height field during the Northern Hemisphere winter. *Mon. Wea. Rev.*, **109**, 784–812.
- Watts, D. J., and S. H. Strogatz, 1998: Collective dynamics of ‘small-world’ networks. *Nature*, **393**, 440–442.